AIP | Applied Physics Letters

Photoreflectance spectroscopy of GaInSbBi and AlGaSbBi quaternary alloys

J. Kopaczek, M. K. Rajpalke, W. M. Linhart, T. S. Jones, M. J. Ashwin, R. Kudrawiec, and T. D. Veal

Citation: Applied Physics Letters **105**, 112102 (2014); doi: 10.1063/1.4895930
View online: http://dx.doi.org/10.1063/1.4895930
View Table of Contents: http://scitation.aip.org/content/aip/journal/apl/105/11?ver=pdfcov
Published by the AIP Publishing

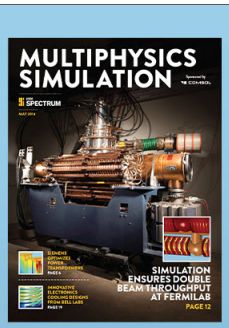

Photoreflectance spectroscopy of GaInSbBi and AlGaSbBi quaternary alloys

J. Kopaczek,[1,2,a)] M. K. Rajpalke,[2,a)] W. M. Linhart,[2] T. S. Jones,[3] M. J. Ashwin,[3] R. Kudrawiec,[1] and T. D. Veal[2,b)]
[1]*Institute of Physics, Wrocław University of Technology, Wybrzeże Wyspiańskiego 27, 50-370 Wrocław, Poland*
[2]*Stephenson Institute for Renewable Energy and Department of Physics, School of Physical Sciences, University of Liverpool, Liverpool L69 7ZF, United Kingdom*
[3]*Department of Chemistry, University of Warwick, Coventry CV4 7AL, United Kingdom*

(Received 30 July 2014; accepted 4 September 2014; published online 16 September 2014)

Molecular beam epitaxy is used to grow $Ga_{1-y}In_ySb_{1-x}Bi_x$ ($y \leq 5.5\%$ and $x \leq 2.5\%$) and $Al_yGa_{1-y}Sb_{1-x}Bi_x$ alloys ($y \leq 6.6\%$ and $x \leq 2.0\%$). The alloy composition and film thickness are determined by high resolution x-ray diffraction. The band gap of the alloys is determined by photomodulated reflectance (PR) spectroscopy. The band gap energy reduces with increasing In and Bi contents and decreasing Al content. The band gap energy reduction between 15 and 290 K is in the range of 60–75 meV, somewhat lower than the 82 meV for GaSb. The broadening of the band gap-related PR feature is between 16 and 28 meV. © *2014 Author(s). All article content, except where otherwise noted, is licensed under a Creative Commons Attribution 3.0 Unported License*. [http://dx.doi.org/10.1063/1.4895930]

The incorporation of a dilute amount of Bi in III–V semiconductors has shown great potential due to the Bi-induced band gap reduction and enhanced spin-orbit splitting.[1–3] While the growth and properties of III-AsBi alloys have been well-researched over the past decade, studies of GaSbBi alloys are in their infancy in spite of GaSb-based alloys being very promising for optoelectronics applications, such as high power lasers, operating in the important 2–5 μm (0.62–0.25 eV) range. The earliest reported growth of GaSbBi alloys achieved low Bi incorporation of up to only 0.8% (Refs. 4 and 5) and lattice contraction with respect to the substrate.[5] More recently, GaSbBi alloys have been grown with up to 9.6% Bi incorporation on the anion sublattice.[6,7] The Bi content in these high quality GaSbBi alloys, with greater than 99% substitutional Bi, was controlled by varying the growth temperature and growth rate. Optical absorption, photoreflectance, and photoluminescence measurements showed band gap reduction with Bi incorporation of ~30–36 meV/%Bi.[6,8,9] Initial indications, from calculations separately employing k·P methods[6] and density functional theory,[10] suggest that the band gap reduction is largely due to downward shift of the conduction band minimum (~26 meV/%Bi) due to Bi 6*s* states, but with some upward shift of the valence band maximum (~10 meV/%Bi) due to an anticrossing interaction between the GaSb valence bands and the Bi 6*p* states.

Here, quaternary gallium-rich antimonide bismide alloys are studied, in contrast to previous reports of indium-rich InGaSbBi alloys.[11,12] One advantage of alloying with In and Al is that it provides a method of achieving different band offsets for tuning the properties of quantum well device structures. The substitution of In into GaSb decreases the band gap with the reduction being entirely due to a downward shift of the conduction band minimum (CBM). Therefore, In and Bi provide complementary methods of reducing the band gap of GaSb; due to the negligibly small valence band offset between GaSb and InSb,[13] In only lowers the CBM energy, enhancing electron confinement, while Bi shifts the CBM down and the valence band maximum (VBM) up in energy,[6,10] enhancing both electron and hole confinement. Alloying In, Al, and Bi in GaSb all increase the lattice parameter because InSb, AlSb, and GaBi all have lattice constants greater than that of GaSb.[13] In contrast to the effect of In and Bi on the band gap, however, Al increases the band gap by shifting both the CBM up and the VBM down in energy with respect to the GaSb band edges. This makes alloying with Al of interest for barrier layers. Therefore, GaInSbBi and AlGaSbBi quaternary alloys are of interest to offer flexibility in band gap and band offset tuning in the mid-infrared in addition to what is already available from conventional III–V semiconductor alloys and dilute nitride antimonides.[14–19] In particular, GaSb-based dilute bismide alloys may offer a means of overcoming the limitations of GaInAsSb alloys[20] for achieving high continuous wave output power laser diodes at wavelengths beyond 2.7 μm at room temperature.

In this Letter, the structural and optical properties of GaInSbBi and AlGaSbBi quaternary alloys grown by molecular-beam epitaxy (MBE) are presented. High resolution x-ray diffraction (HRXRD) is used to determine the In, Al, and Bi incorporation in the epilayers. The optical properties of the alloys are studied using photoreflectance (PR) spectroscopy. The temperature dependent band gap variation is studied for GaInSbBi and AlGaSbBi alloys with different In, Al, and Bi contents.

The GaInSbBi and AlGaSbBi epilayers were grown on undoped (001) GaSb substrates by solid-source MBE at a nominal growth rate of 1.0 μm h^{-1}. The sources and substrate preparation procedures are described elsewhere.[6] A GaSb buffer layer of 100 nm thickness was grown at 500 °C and substrates were cooled to 275 °C. Before the growth of GaInSbBi, a layer of GaInSb was grown with a thickness of

[a)]J. Kopaczek and M. K. Rajpalke contributed equally to this work.
[b)]Electronic mail: T.Veal@liverpool.ac.uk

approximately 100 nm. This layer was used to determine the Ga:In ratio. Each GaInSbBi layer was then grown to a nominal thickness of 300 nm using the same Ga and In fluxes as for the GaInSb layer and the Bi content was determined under the assumption that incorporating Bi does not significantly change the Ga:In ratio. An AlGaSb "calibration" layer was used when the AlGaSbBi films were grown. Films of $Ga_{1-y}In_ySb_{1-x}Bi_x$ and $Al_yGa_{1-y}Sb_{1-x}Bi_x$ alloys with different compositions were grown by keeping the Sb and Bi fluxes constant for all the samples but varying the Ga, In, and Al fluxes to maintain a constant total group III flux and constant V:III ratio. The group III cells were characterized using reflection high energy electron diffraction oscillations and XRD as a function of cell temperature. The Bi beam equivalent pressure flux was set to approximately 3.3×10^8 mbars using the beam monitoring ion gauge.

The structural characterization was carried out by HRXRD using a Philips X'Pert diffractometer equipped with a Cu $K\alpha_1$ x-ray source ($\lambda = 0.15406$ nm) with a four bounce Ge (220) monochromator. For the purpose of determining PR temperature dependence, samples were mounted on a cold finger in a helium closed cycle refrigerator coupled with a programmable temperature controller, allowing measurements in the 15–290 K temperature range. A single grating 0.55 m focal-length monochromator and a thermoelectrically cooled InGaAs *pin* photodiode were used to disperse and detect the reflected light from the samples. A 150 W tungsten-halogen bulb was used as the probe, and a semiconductor laser (660 nm line) was used as the pump source. The probe and pump beams were focused onto the sample to a diameter of ~3 mm and the power of laser beam was reduced to 20 mW using a neutral density filter. The pump beam was modulated by a mechanical chopper at a frequency of 280 Hz. Phase sensitive detection of the PR signal was accomplished using a lock-in amplifier.

HRXRD ω–2θ scans from 004 planes for the as-grown GaInSbBi samples with GaInSb calibration layers, along with the GaSb substrates are shown in Fig. 1. The main peak at 36.3606° corresponds to the GaSb substrate, while the highest intensity peaks at lower angles correspond to the

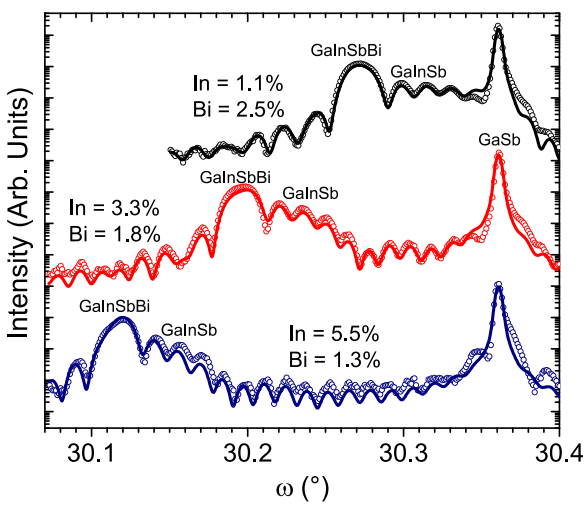

FIG. 1. XRD ω-2θ scans of GaInSbBi films grown on GaSb(001) substrates. To enable comparison with the dynamical simulations (solid lines) only every second experimental data point is shown.

GaInSbBi alloys. The GaInSb layer manifests itself as enhanced intensity on the high angle side of the GaInSbBi peak. The GaInSb feature and GaInSbBi peak positions shift to lower Bragg angle with increasing In cell temperature. The 004 reflections and the Pendellösung fringes were modeled by dynamical simulations, in order to calculate the lattice constants and the layer thickness of the GaInSb and GaInSbBi alloys. The thicknesses of the quaternary III-SbBi epilayers determined from dynamical simulation are given in Table I. The epilayer XRD peaks at lower angle than the substrate correspond to the expected expansion of the lattice upon incorporation of In and Bi, just as reported recently for Bi incorporation in GaSb,[6,7] but in contrast to earlier reports of lattice contraction upon incorporation of Bi in GaSb and InSb.[5,21,22]

Fig. 2 shows the ω-2θ scans for AlGaSbBi samples grown on GaSb, along with AlGaSb calibration layer. The AlGaSb feature and AlGaSbBi peak positions shift to lower Bragg angle with increasing Al cell temperature. Expansion of the lattice is observed for the AlGaSb and AlGaSbBi films with respect to the GaSb substrate.

Asymmetric 115 reciprocal space maps (RSM) were performed (not shown here) to study the strain state of the GaInSbBi and AlGaSbBi epilayers. The asymmetric maps revealed that the $Ga_{1-y}In_ySb_{1-x}Bi_x$ and $Al_yGa_{1-y}Sb_{1-x}Bi_x$ layers are completely strained to the GaSb in-plane lattice constant. The presence of interference fringes also indicates the pseudomorphic nature of the epitaxy with excellent crystalline quality.

The relaxed lattice constants are obtained by correcting the XRD data for the tetragonal distortion of the GaInSbBi and AlGaSbBi using the elastic constants of GaSb under the assumption that they do not change significantly for small percentages of In, Al, and Bi.[6,13,23] Using Vegard's law, the In, Al, and Bi contents are calculated using lattice constant values of 6.0959 Å for GaSb, 6.4794 Å for InSb, 6.1355 Å for AlSb, and 6.3417 Å for AlBi.[13,25] The values for the zinc blende GaBi and InBi lattice constants used in the calculations of 6.272 Å and 6.626 Å, respectively, are determined by extrapolating the $GaSb_{1-x}Bi_x$ and $InSb_{1-x}Bi_x$ lattice constants as a function of Rutherford backscattering-determined Bi content to $x = 1$.[7,24] (The RBS Bi contents used are those corresponding to beneath any surface Bi droplets on the InSbBi films.[24]) The In and Bi contents in the $Ga_{1-y}In_ySb_{1-x}Bi_x$ layers in order of increasing In cell temperature were found to be y = 1.1%, 3.3%, 5.5% and x = 2.5%, 1.8%, 1.3% of Bi, respectively. The Al and Bi contents in the $Al_yGa_{1-y}Sb_{1-x}Bi_x$ layers in order of increasing Al cell temperature were found to be y = 1.6%, 6.6% and x = 2.0%, 1.4%, respectively. These results suggest that, for the range of alloying on the cation sublattice considered here, the presence of In and Al suppresses Bi incorporation when compared with the growth of GaSbBi alloys.

Figures 3(a) and 3(b) show PR spectra measured at 15 K for $Ga_{1-y}In_ySb_{1-x}Bi_x/Ga_{1-y}In_ySb$ and $Al_yGa_{1-y}Sb_{1-x}Bi_x/Al_yGa_{1-y}Sb$ samples, respectively. For the $Ga_{1-y}In_ySb_{1-x}Bi_x/Ga_{1-y}In_ySb$ samples, two PR resonances are clearly visible below the GaSb energy gap. One of them is associated with the E_0 transition in the GaInSb layer, and it redshifts with increasing In concentration. The second

TABLE I. Varshni and Bose-Einstein parameters extracted from fitting of the E_0 transition shown in Fig. 5 by the Varshni expression, $E_0(T) = E_0(0) - [\alpha T^2/(\beta + T)]$, where $E_0(0)$ is the band gap energy at $T = 0$ K, while α and β are the so-called Varshni coefficients, and the Bose-Einstein expression, $E_0(T) = E_0(0) - [2a_B/(\exp(\theta_B/T) - 1)]$, where a_B is the strength of the electron-average phonon interaction and θ_B is the average phonon temperature.

	Varshni			Bose-Einstein		
Alloy (thickness)	$E_0(0)$ (eV) ± 0.001	α (10^{-4} eV/K)	β (K)	$E_0(0)$ (eV) ± 0.001	a_B (meV)	θ_B (K)
GaSb[a]	0.813	3.78	94	0.811	22	127
$GaSb_{0.979}Bi_{0.021}$[b]	0.740	3.7 ± 0.5	110 ± 50	0.738	46 ± 5	220 ± 50
$In_{0.53}Ga_{0.47}Bi_{0.021}As_{0.979}$[c] (360 nm)	0.729	4.1 ± 0.6	225 ± 70	0.727	34 ± 4	208 ± 20
$Ga_{0.945}In_{0.055}Sb$[d] (100 nm)	0.754	3.3 ± 0.5	147 ± 20	0.753	20 ± 3	157 ± 20
$Ga_{0.967}In_{0.033}Sb$[d] (110 nm)	0.758	3.9 ± 0.5	225 ± 80	0.756	30 ± 5	221 ± 40
$Ga_{0.945}In_{0.055}Sb_{0.987}Bi_{0.013}$[d](260 nm)	0.721	3.7 ± 0.2	190 ± 40	0.719	29 ± 2	188 ± 10
$Ga_{0.967}In_{0.033}Sb_{0.982}Bi_{0.018}$[d] (275 nm)	0.729	4.2 ± 0.5	296 ± 60	0.727	41 ± 3	236 ± 20
$Ga_{0.989}In_{0.011}Sb_{0.975}Bi_{0.025}$[d] (275 nm)	0.737	3.8 ± 0.5	240 ± 80	0.735	30 ± 5	200 ± 40
$Ga_{0.934}Al_{0.066}Sb_{0.986}Bi_{0.014}$[d] (300 nm)	0.872	4.2 ± 0.5	234 ± 40	0.870	38 ± 3	200 ± 20
$Ga_{0.984}Al_{0.016}Sb_{0.980}Bi_{0.020}$[d] (285 nm)	0.772	4.1 ± 0.5	240 ± 80	0.770	38 ± 3	234 ± 20

[a]Reference 13.
[b]Reference 8.
[c]Reference 27.
[d]This work.

resonance is attributed to the E_0 transition in the GaInSbBi layer. Also two PR resonances are observed for the $Al_yGa_{1-y}Sb_{1-x}Bi_x/Al_yGa_{1-y}Sb$ samples. The higher energy resonance is attributed to the E_0 transition in the AlGaSb layer and the lower energy resonance to the E_0 transition in the AlGaSbBi layer. It is clearly visible that the resonances redshift with increasing Bi and decreasing Al concentrations.

In order to determine the energy of the E_0 transition and its broadening, the PR spectra were fitted using the Aspnes formula[26] as described in Ref. 8. Examples of experimental data fitted by the Aspnes formula are shown in Fig. 3 together with the moduli of PR resonances which are shown as dashed black lines. The moduli of PR resonances were obtained from the fit using the method described in Ref. 8.

Figure 4 shows the temperature dependencies of the PR spectra measured for the GaInSbBi and AlGaSbBi samples at the same conditions of band bending modulation. It is distinctly apparent that the E_0 transition in the GaInSbBi, GaInSb, AlGaSbBi, and GaAlSb layers redshifts and broadens with increasing temperature.

The temperature dependence of the energy of the E_0 transition extracted from the fitting procedure is shown in

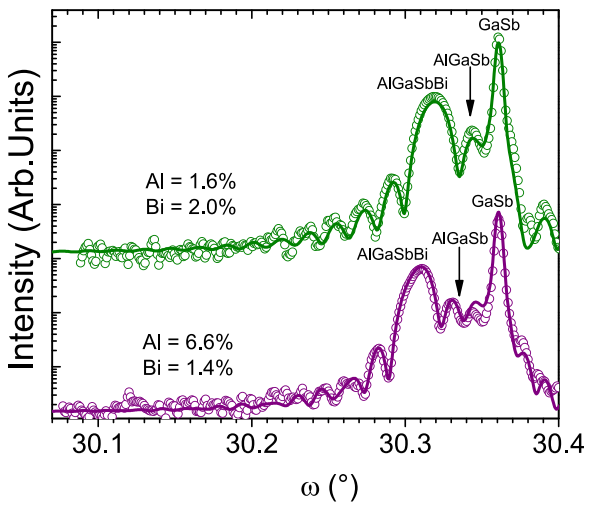

FIG. 2. XRD ω-2θ scans of AlGaSbBi films grown on GaSb(001) substrates. To enable comparison with the dynamical simulations (solid lines) only every second experimental data point is shown.

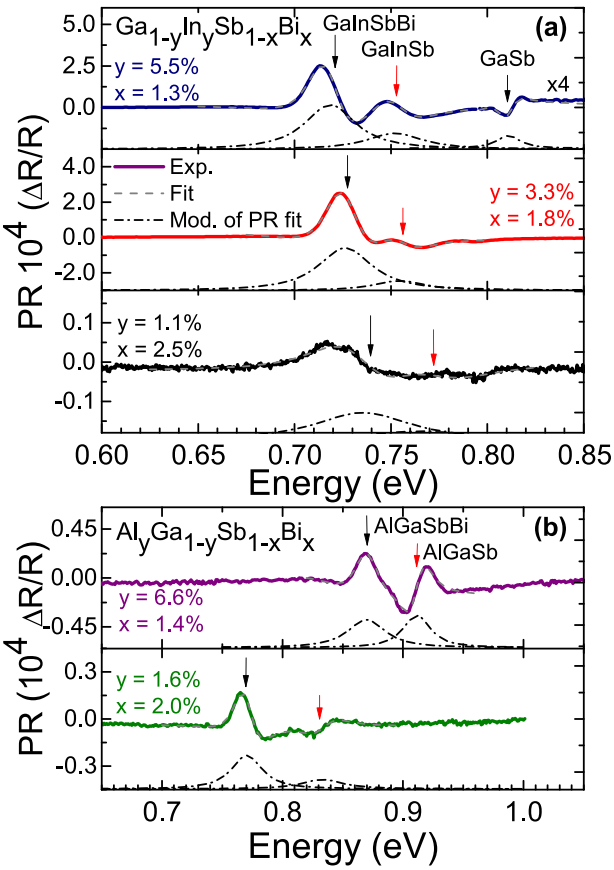

FIG. 3. Photoreflectance spectra obtained at 15 K of (a) $Ga_{1-y}In_y Sb_{1-x}Bi_x$ layers with y = 5.5%, 3.3%, 1.1% of In and x = 1.3%, 1.8%, 2.5% of Bi and (b) $Ga_{1-y}Al_ySb_{1-x}Bi_x$ layers with y = 6.6%, 1.6% of Al and x = 1.4%, 2.01% of Bi, together with the fitting curves (dashed grey lines) in the vicinity of energy gap transition and the moduli of photoreflectance resonance (dashed-dotted lines).

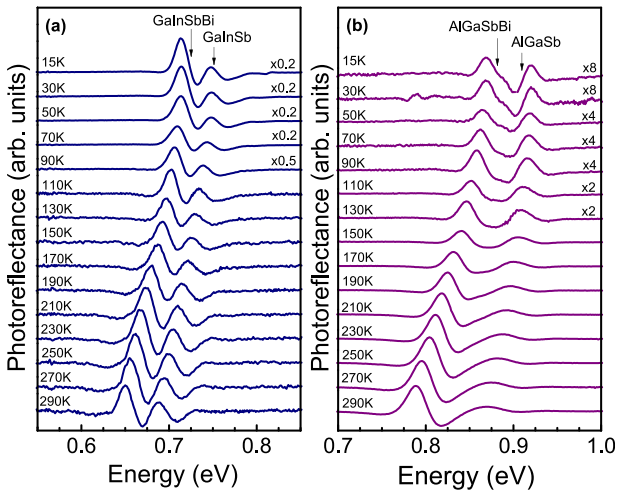

FIG. 4. Temperature dependence of photoreflectance spectra of (a) 260 nm of $Ga_{0.945}In_{0.055}Sb_{0.987}Bi_{0.013}$ on 110 nm of $Ga_{0.945}In_{0.055}Sb$ and (b) 300 nm of $Ga_{0.934}Al_{0.066}Sb_{0.986}Bi_{0.014}$ on 105 nm of $Ga_{0.934}Al_{0.066}Sb$ in the vicinity of E_0 transition.

Figure 5 for the three GaInSbBi and two AlGaSbBi samples of various compositions. For the sample of composition $Ga_{0.989}In_{0.011}Sb_{0.975}Bi_{0.025}$, no clear E_0 PR feature is apparent above 200 K. On this figure, the temperature dependence of the band gap of GaSb is also plotted. It is apparent that the temperature induced narrowing of the band gap in GaInSbBi and AlGaSbBi alloys is significant (between ~60 and 75 meV in the range of 15–290 K), comparable with other narrow gap dilute bismides and somewhat less than the 82 meV observed for GaSb.[8,13,27] The temperature dependence of the E_0 transition is fitted using both the Varshni[28] and Bose-Einstein-type[13,29,30] expressions that are given in the caption of Table I.

The dashed and solid lines in Fig. 3 correspond to fitting curves of experimental points by the Varshni and Bose-Einstein expressions, respectively. The fit-determined parameters, $E_0(0)$, α, β, a_B, and θ_B, for the E_0 transition are listed in Table I. In addition, the literature data for GaSb from Ref. 13 are also given in Table I.

The Varshni and Bose-Einstein parameters determined for the E_0 transition for the GaInSbBi and AlGaSbBi samples

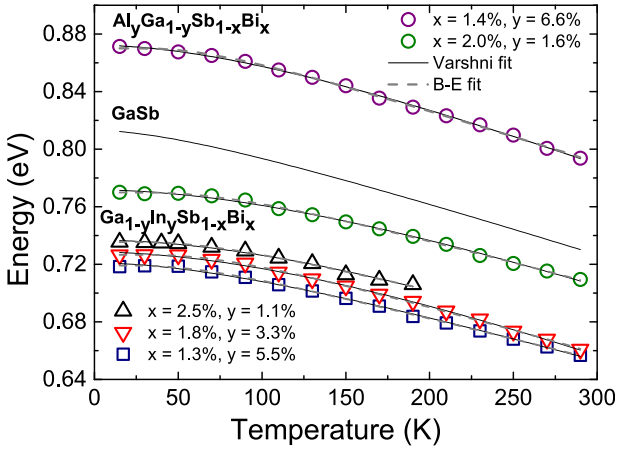

FIG. 5. Temperature dependence of E_0 transition energy for GaInSbBi and AlGaSbBi alloys together with fits by the Varshni (solid lines) and Bose-Einstein (dashed lines) formulae.

were compared with values obtained for other dilute bismide alloys from Refs. 8 and 27. It can be concluded that they are similar and consistent, taking into account their errors. Analysis of the Bose-Einstein parameters indicates that Bi incorporation into III–V alloys enhances the strength of the electron-average phonon interaction and the average phonon temperature, as noted previously in Ref. 8.

From the fitting procedure, information about the broadening of the E_0 transition is also obtained. In the case of the GaInSbBi samples, the values of broadening are comparable for all the samples and are in the range ~16–24 meV, increasing with increasing temperature. For the AlGaSbBi alloys, values in the range ~16–24 meV were obtained for the sample with Bi = 2.0% and Al = 1.6% and ~21–28 meV for the sample with Bi = 1.4% and Al = 6.6%, again with the broadening increasing for the higher temperatures.

For GaSbBi, the band gap reduction upon incorporation of Bi is about 30 meV/%Bi at 15 K. The set of quaternary antimonide bismide alloys investigated here provides an initial indication of the influence of alloying with In and Al on the Bi-induced band gap reduction. Comparison of the E_0 PR feature for the GaInSb and GaInSbBi layers for each Ga:In ratio suggests the Bi-induced band gap reduction is smaller than for GaSbBi alloys. However, as there is only one Bi-content for each In-content, this result should be considered to be provisional. Comparison of the E_0 PR feature for the AlGaSb and AlGaSbBi layers, on the other hand, indicates very similar band gap reduction per %Bi as for GaSbBi. This tentatively implies that alloying with up to 6.6% Al has little or no effect on the Bi-induced band gap reduction.

In conclusion, the epitaxial growth and photoreflectance of $Ga_{1-y}In_ySb_{1-x}Bi_x$ ($y \leq 5.5\%$ and $x \leq 2.5\%$) and the $Al_yGa_{1-y}Sb_{1-x}Bi_x$ alloys ($y \leq 6.6\%$ and $x \leq 2.0\%$) have been investigated. High resolution x-ray diffraction was used to determine the alloy composition and film thickness. The GaInSbBi alloys show redshift of the E_0 band gap-related transition with increasing In and Bi contents, whereas the AlGaSbBi layers show redshift with increasing Bi and *decreasing* Al content. The temperature induced narrowing of the band gap in GaInSbBi and AlGaSbBi alloys is significant (between ~60 and 75 meV) in the range of 15–290 K, but slightly less than that observed for GaSb. The Varshni and Bose-Einstein parameters determined for the E_0 transition of the GaInSbBi and AlGaSbBi samples are similar to the values obtained for other dilute bismide alloys.

The work at Liverpool and Warwick was supported by the University of Liverpool, the University of Warwick, and the Engineering and Physical Sciences Research Council (EPSRC) under Grant Nos. EP/G004447/2 and EP/H021388/1, and the work at Wroclaw by the NCN (Grant No. 2012/07/E/ST3/01742).

[1]S. Francoeur, M.-J. Seong, A. Mascarenhas, S. Tixier, M. Adamcyk, and T. Tiedje, Appl. Phys. Lett. **82**, 3874 (2003).
[2]X. Lu, D. A. Beaton, R. B. Lewis, T. Tiedje, and Y. Zhang, Appl. Phys. Lett. **95**, 041903 (2009).
[3]B. Fluegel, S. Francoeur, A. Mascarenhas, S. Tixier, E. C. Young, and T. Tiedje, Phys. Rev. Lett. **97**, 067205 (2006).
[4]S. K. Das, T. D. Das, S. Dhar, M. de la Mare, and A. Krier, Infrared Phys. Technol. **55**, 156 (2012).

[5]Y. Song, S. Wang, I. S. Roy, P. Shi, and A. Hallen, J. Vac. Sci. Technol., B **30**, 02B114 (2012).
[6]M. K. Rajpalke, W. M. Linhart, M. Birkett, K. M. Yu, D. O. Scanlon, J. Buckeridge, T. S. Jones, M. J. Ashwin, and T. D. Veal, Appl. Phys. Lett. **103**, 142106 (2013).
[7]M. K. Rajpalke, W. M. Linhart, M. Birkett, K. M. Yu, J. Alaria, J. Kopaczek, R. Kudrawiec, T. S. Jones, M. J. Ashwin, and T. D. Veal, J. Appl. Phys. **116**, 043511 (2014).
[8]J. Kopaczek, R. Kudrawiec, W. M. Linhart, M. K. Rajpalke, K. M. Yu, T. S. Jones, M. J. Ashwin, J. Misiewicz, and T. D. Veal, Appl. Phys. Lett. **103**, 261907 (2013).
[9]J. Kopaczek, R. Kudrawiec, W. M. Linhart, M. K. Rajpalke, T. S. Jones, M. J. Ashwin, and T. D. Veal, "On the nature of low and high energy photoluminescence from $GaSb_{1-x}Bi_x$ with $0 < x < 0.042$," Appl. Phys. Express. (submitted).
[10]M. Polak, P. Scharoch, R. Kudrawiec, J. Kopaczek, M. Winiarski, W. Linhart, M. Rajpalke, K. M. Yu, T. S. Jones, M. J. Ashwin, and T. D. Veal, J. Phys. D: Appl. Phys. **47**, 355107 (2014).
[11]Y. Hayakawa, M. Ando, T. Matsuyama, E. Hamakawa, T. Koyama, S. Adachi, K. Takahashi, V. G. Lifshits, and M. Kumagawa, J. Appl. Phys. **76**, 858 (1994).
[12]Q. Du, J. Alperin, and W. I. Wang, J. Cryst. Growth **175–176**, 849 (1997).
[13]I. Vurgaftman, J. R. Meyer, and L. R. Ram-Mohan, J. Appl. Phys. **89**, 5815 (2001).
[14]L. Buckle, B. R. Bennett, S. Jollands, T. D. Veal, N. R. Wilson, B. N. Murdin, C. F. McConville, and T. Ashley, J. Cryst. Growth **278**, 188 (2005).
[15]P. H. Jefferon, T. D. Veal, L. F. J. Piper, B. R. Bennett, B. N. Murdin, L. Buckle, G. W. Smith, and T. Ashley, Appl. Phys. Lett. **89**, 111921 (2006).
[16]D. Wang, S. P. Svensson, L. Shterengas, G. Belenky, C. S. Kim, I. Vurgaftman, and J. R. Meyer, J. Appl. Phys. **105**, 014904 (2009).
[17]M. J. Ashwin, T. D. Veal, J. J. Bomphrey, I. R. Dunn, D. Walker, P. A. Thomas, and T. S. Jones, AIP Adv. **1**, 032159 (2011).
[18]M. J. Ashwin, D. Walker, P. A. Thomas, T. S. Jones, and T. D. Veal, J. Appl. Phys. **113**, 033502 (2013).
[19]J. J. Mudd, N. J. Kybert, W. M. Linhart, L. Buckle, T. Ashley, P. D. C. King, T. S. Jones, M. J. Ashwin, and T. D. Veal, Appl. Phys. Lett. **103**, 042110 (2013).
[20]A. Joullié, P. Christol, A. N. Baranov, and A. Vicet, "Mid-infrared 2–5 μm heterojunction laser diodes" in *Solid-State Mid-Infrared Laser Sources*, Topics in Applied Physics Vol. 89, edited by I. T. Sorokina and K. L. Vodopyanov (Springer, 2003), pp. 1–61.
[21]J. J. Lee and M. Razeghi, Opto-Electron. Rev. **6**, 25 (1998).
[22]Y. Song, S. Wang, I. S. Roy, P. Shi, A. Hallen, and Z. Lai, J. Cryst. Growth **378**, 323 (2013).
[23]M. J. Ashwin, R. J. H. Morris, D. Walker, P. A. Thomas, M. G. Dowsett, T. S. Jones, and T. D. Veal, J. Phys. D: Appl. Phys. **46**, 264003 (2013).
[24]M. K. Rajpalke, W. M. Linhart, K. M. Yu, J. Alaria, J. J. Bomphrey, T. S. Jones, M. J. Ashwin, and T. D. Veal, "Bi-induced band gap reduction in epitaxial InSbBi alloys," Appl. Phys. Lett. (submitted).
[25]P. Carrier and S. H. Wei, Phys. Rev. B **70**, 035212 (2004).
[26]D. E. Aspnes, Surf. Sci. **37**, 418 (1973).
[27]R. Kudrawiec, J. Kopaczek, J. Misiewicz, W. Walukiewicz, J. P. Petropoulos, Y. Zhong, P. B. Dongmo, and J. M. O. Zide, J. Appl. Phys. **112**, 113508 (2012).
[28]Y. P. Varshni, Physica **34**, 49 (1967).
[29]S. Logothetidis, M. Cardona, P. Lautenschlager, and M. Garriga, Phys. Rev. B **34**, 2458 (1986).
[30]P. Lautenschlager, M. Garriga, S. Logothetidis, and M. Cardona, Phys. Rev. B **35**, 9174 (1987).